Abnormal expressions of inflammatory-related mediators and inhibition of fat metabolism in mice infected with influenza a virus

MinYao[1], Li Wang[2], Dengbing Yao[3] and Dengfu Yao[4]*

[1]Department of Immunology,Medical School, Nantong University, Jiangsu, China
[2]Department of Medical Informatics,MedicalSchool, Nantong University, Jiangsu, China
[3]Key Lab. of Neuroregeneration, Nantong University, Jiangsu, China
[4]AffiliatedHospitalof Nantong University, Jiangsu, China

Abstract: The pathophysiological role of influenza infection is poorly understood. In this study, one non-neurovirulent virus (IAV/Aichi/2/68/H3N2) strain was used to infect intra-nasally mice at different age to investigate the mechanism of cerebral edema formation and lower activities of mitochondria enzymes after influenza A virus (IAV) infection. Mice suffered 46.4% mortality in newborn compared with 96.0% in weanling, 100% in adult on day 7, respectively. IAV-RNA was easily detected in the brain of newborn mice. Significant production of endothelin-1 and inducible nitric oxide syntheses were increased on the 3rd and 5th day after IAV infection, associated with increasing blood-brain barrier permeability, brain edema formation and the higher mortality of animals. Production of tumor necrosis factor-α was related to inhibition of mitochondrial enzyme activities, suggesting that over expression of inflammatory cytokines and lower enzyme activities in mitochondria after IAV infection.

Keywords: Virus infection, fat metabolism, cytokines, carnitine and mice.

INTRODUCTION

Influenza A virus (IAV) is the most important cause of respiratory illness. Its impact is universal, affecting persons worldwide. In children, IAV infection primarily affects the upper respiratory tract, followed by an acute and diffuse inflammation of the bronchoalveolar tract (Vogel *et al*., 2014). Clinically, its infections are accompanied by production of endogenous pyrogens, high fever, malaise, neurologic complication, and results in host cell death by cytolytic or apoptotic mechanisms, with epithelial cells and leukocytes producing chemokines, proinflammatory and other immunoregulatory cytokines (Sawadogo *et al*., 2006 and Momtaz *et al*., 2010). Much attention has been paid to the multiple functions of endothelin (ET) isopeptides (ET-1~3), potent vaso-constrictors of vascular smooth muscle in brain edema formation. In the brain, ETs and their receptors that localize in neurons, glial cells, and microvessel endothelial cells have been implicated in physiological and patho-physiological roles by modulating neuronal functions or regulating cerebral blood flow and metabolism (McAuley *et al*., 2013). Topical ET-1 can reduce cerebral blood flow and induce neuronal damage. Disruption of blood-brain barrier (BBB) and edema are induced with the progression of brain injury. Recently, it has been suggested that ETs regulate BBB functions. ET-1 enhances the permeability of BBB. These findings may implicate ET-1 in the pathogenesis of brain edema accompanying cerebrovascular disorders, but the precise mechanisms are unclear (Yao D *et al*., 2011). Invasion by a non-neurovirulent epidemic IAV in capillaries with progressive brain edema have been observed previously shown that after intranasal infection of mice having impaired mitochondrial fatty acid metabolism congenitally or posteriorly in the newborn periods. Carnitine-deficient mice exhibited higher virus-genome numbers in the brain, accumulation of virus antigen in the capillaries and increased brain vascular permeability compared to in wild type mice. Mini-plasmin potentiates viral-multiplication and destroys BBB and IAV infection may affect the BBB increasing permeability (Yao M *et al*., 2011). However, such minor injury may be detected by presently available techniques and a few studies have analyzed the role of ETs on BBB dysfunction and edema in experimental encephalitis. Thus, the aims of this study were to evaluate the expressions of ETs and cytokines and effects of fat metabolism after IAV infection.

MATERIALS AND METHODS

Mice and animal model

Homozygote C_{57}BL/6 ($^{wt/wt}$, WT) mice were used, and housed under bio-clean conditions at 22±2℃ environment with a 12-hr light/dark cycle and 55% humidity. Mice-adapted influenza A/Aichi/2/68 (H3N2) virus was propagated in 11-d-old embryonated chicken eggs. Infected dose were measured in WT mice with serial 10-fold dilutions of virus. The newborn (2nd day), weanling (3-wk-old) and adult mice (8-wk-old) were lightly anaesthetized with ether for 1 min and followed by intranasal infection with 1.2, 3.3 and $6.6x10^4$ plaque-forming unit (PFU) of the virus in PBS administered

*Corresponding author: e-mail: yaodf@ahnmc.com

through nostrils, respectively. Mice were treated twice a day a subcutaneous injection of a clinical dose (2mg/kg) of diclofenac sodium (Sigma, St. Louis. M.D.). Mice were then monitored daily for survival and weight loss, recorded their clinical signs and sacrificed at different time. All procedures performed on the animals were conducted in accordance with the guidelines for experimental animals approved by the Animal Care and Use Committee of Tokushima University, Japan.

Measurement of tissue ETs level

To measure immunoreactive ETs content, brain and lung samples after IAV infection were immediately frozen in liquid nitrogen, weighed, and stored at -80^{o}C until ET extraction. Tissues were homogenized with sonication for 1min in 0.5ml of 0.6N HCl containing 0.1%TFF for inactivate proteases. The homogenates were centrifuged at 15 000rpm for 20 min at 4^{o}C. The supernatants (1.0ml) were extracted on 100mg Amprep C2 column pretreatment sequentially with 3 ml of MeOH, 3.0ml of distill water and 3.0ml of 0.1% of TFA. The columns were washed with 4ml of 0.1% TFA and 4ml of 20% CAN/0.1% TFA. ET was eluted by 1.0ml of 60% CAN, 0.1% TFA and concentrated to 200~300µl under reduced pressure by speedvac for 1 hr. The concentrations of tissue ET-1 were analyzed with ELISA kits. Brain ET-1 content was measured in complete sham-operated rats immediately after the operation.

Analysis of TNF-α level

Brain tissues of IAV-infected mice on days 3 and 5 in this study were homogenized for 1min in PBS (0.1 M, pH 8.0) at 4^{o}C and then centrifuged for 10min at 5000 rpm at 4^{o}C. TNF-α concentration in supernatant was determined by an immunoassay kit for mouse TNF-α (BioSource International, Inc. California USA), according to the manufacturer's instructions, samples were measured in triplicates.

Water content in brain

To measure brain water content, the infected mice were sacrificed at different time after IAV infection. The brain samples were dried in an oven at 130^{o}Cfor 6 hr. The water content of these samples was then measured by the wet and dry method as follows: water content (%) = (wet wt-dry wt)x 100/wet wt. Brain water content was also measured in complete sham-operated mouse 24hr after the operation.

BBB permeability for EB

The infected mice on days 3 and 5 were anaesthetized with pentobarbital (5mg/Kg) and then 10 µl of 2% (w/v) Evans' blue dye in saline was injected into the left cardiac ventricle. After injection for 10 min, the whole body was perfused with 5ml of saline through the left cardiac ventricle and then the brains were excised. The extent of leakage of Evans' blue was detected macroscopically, quantified by extraction, and then measured spectrophotometrically at 605 nm as described.

RNA isolation and RT-PCR

IAV replication in organs of mice was examined directly by genome amplification and the organs from the infected mice on the 5th day were put into the RNase-free tubes containing RNAlater (Ambion, TX, USA). Total RNA was extracted with TRIzol reagent (Gibco BRL) and the random primer and total RNA (1µg/µl) were used to generate cDNA with reverse transcriptase (Gibco BRL). Nested-PCR was amplified for IAV (H3N2 strain) hemagglutinin and their primers and product sizes were summarized in table 1. The final PCR products (232 bp) were sequenced by Taq Dye Terminator method (Applied Bio-systems).

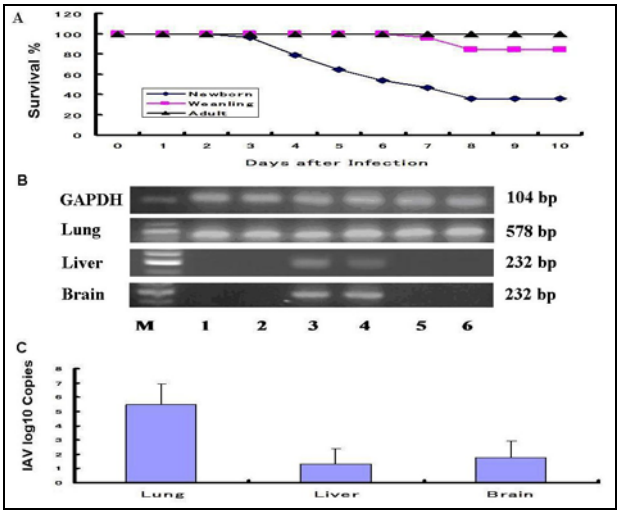

Fig. 1: IAV infection on age-dependency and viral gene analysis A. Newborn (◆, *n*=28), Weanling (■, *n*=25), and Adult (▲, *n*=18) mice were infected with IAV at different loads. Statistical significance was observed in newborn/ suckling mice from the 4th day (p<0.05) in comparing with weanling or adult mice. B Qualitative RT-PCR. Surviving mice on the 5th day were sacrificed, and then brains, lungs and livers were immediately collected for total RNA. One µg of total RNA was subjected to cDNA synthesis, and then nested RT-PCR was carried out. GAPDH: glyceraldehyde-3-phosphate dehydrogenase (104bp) as a control. M, 100bp DNA ladder marker; Lanes 1 & 2: brain RNA of weanling mice; lanes 3 & 4: brain RNA of newborn mice; lanes 5 & 6: brain RNA of adult mice. C Quantitative analysis of virus RNA by real-time PCR (*n*=12). The virus genome copy numbers in the brains, livers and lungs of infected newborn mice.

Measurement of Carnitine and Total NOS Activity

The amounts of free-, short chain acyl- and long chain acyl-carnitine in the brain were determined by means of a radioisotope assay as reported (Cederblad *et al.,* 1972). Measurement of total NOS activity was according to

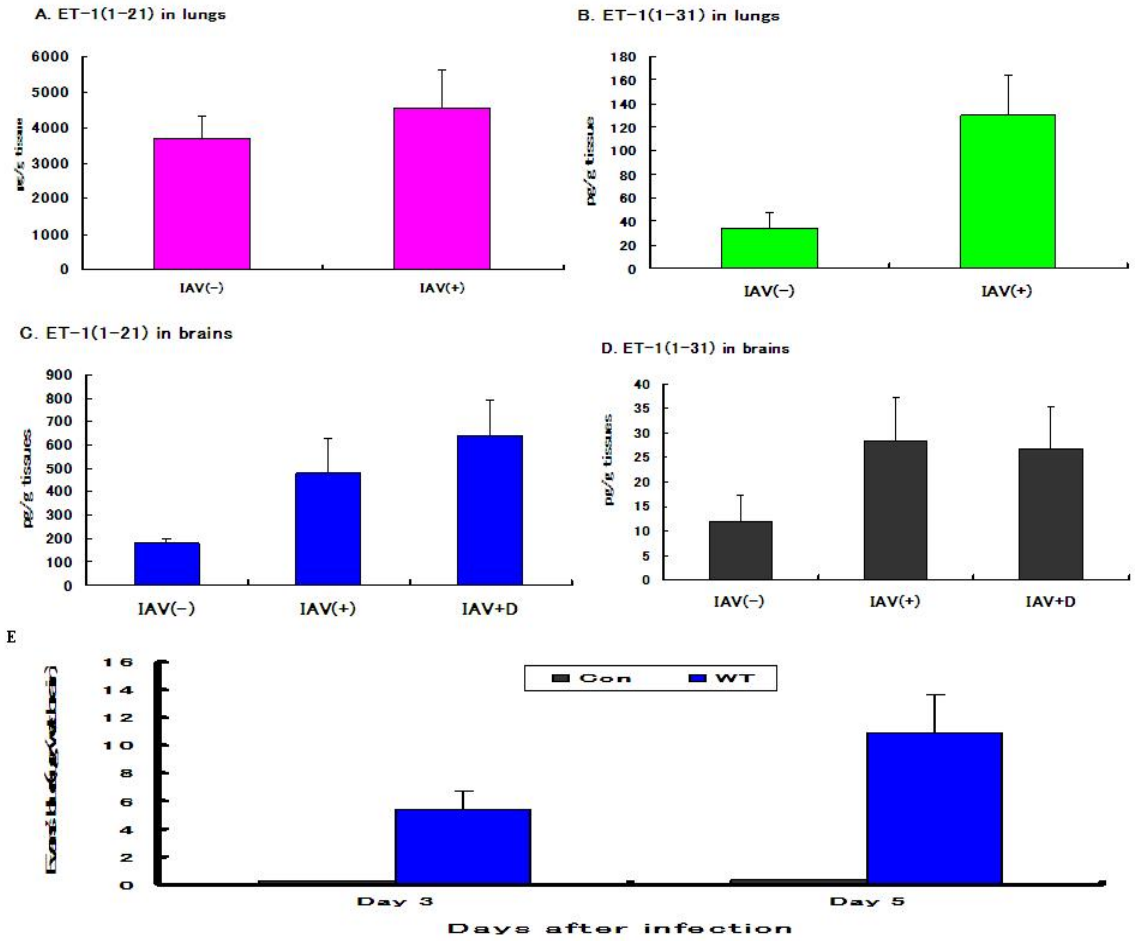

Fig. 2: Expression of ET-1 and BBB-permeability in brains. A~D, ET-1 in brains and effect of diclofenacafter IAV infection. Significant increases of ET-1 (1-31) in lungs, ET-1 (1-21) and ET-1 (1-31) levels (p<0.05) in brains compared with the controls or viral infection with diclofenac treatment. E. Alteration of BBB-permeability in brains of newborn mice on day 3 or 5 was analyzed as described under Methods. Evans' blue levels in the supernatants was the mean ±SD (n=5). Evans' blue levels in the infected mice on day 3 were higher than that in the controlon day 3, p<0.01.

instruction of BIOXYTECH nitric oxide syntheses assay kit (OXIS, OR, USA). Briefly, nitric oxide rapidly degrades to nitrate and nitrite in aqueous solutions. Spectrophotometric quantitation of nitrite using Greiss Reagent is straightforward and sensitive, but it does not measure nitrate, causing a possible under estimation of nitric oxide. The kit employs the NADPH-dependent enzyme nitrate reductase for enzymatic reduction of nitrate to nitrite prior to quantitation of nitrite using Greiss reagent. In acid solution, nitrite is converted to nitrous acid (HNO_2) which diazotizes sulfanilamide. This sulfanilamide-diazonium salt is then reacted with N-(1-Naphthyl)-ethylene-diamine (NED) to produce a chromophore which is measured at 540 nm. This kit can be used to accurately measure as little as 1 µM of nitrite.

STATISTICAL ANALYSIS

Data is expressed as means ± SD and analyzed by Students' *t*test. The differences in mortality among experimental groups were analyzed by means of the Chi-square test. Difference were considered significant at p<0.05.

RESULTS

Virus infection and viral RNA analysis

With IAV inoculations, the respiration of infected mice is markedly increased in rate and depth, movement disorder occurs, neck stiff and severe viral pneumonia was seen after the infected newborn mice death. The newborn mice were infected with IAV successfully and affect markedly the growth of mice. The effects of IAV infection on survival courses of experimental mice were shown in fig. 1A. The neonatal mice showed the different survival curves post inoculation. The survival rate was much lower in newborn mice than those in the weanling- and adult mice. To confirm IAV replication, the genes of IAV

(H3N2 strain) hem agglutinin were examined directly by PCR amplification in lungs of newborn, weanling and adult mice. Infected mice showed a band of 578bp only for the lungs on the first PCR, but one of 232bp was detected for the brains and livers on the nested PCR (fig. 1B). We also used a multiplex TaqMan-based real-time PCR assay with a constructed plasmid containing the HA genome as a standard. The highest numbers of the IAV genome were detected in the lungs in the newborn periods. However, the numbers of the viral genome determined in the livers and brains of mice were significantly higher than control (fig. 1C). The nucleotide sequences of brain and liver IAV gene fragments in the infected mice were identical to those of lung IAV (fig. 1D).

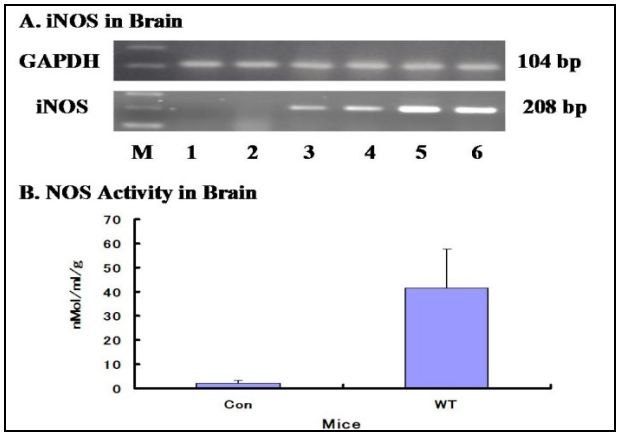

Fig. 3: Expression of cerebral iNOS mRNA and time courses of cerebral edema formation. A. Time courses of cerebral iNOS mRNA expression during IAV infection fragments of iNOS gene were analyzed by RT-PCR. Line 1 & 2 the 1st day after IAV infection, no positive band can be detected; line 3 & 4 the 3rd day after IAV infection, weaker positive band of iNOS gene can be detected and line 5 & 6, stronger positive band can been seen on the 5th day. B. Analysis of total cerebral NOS activity on the 5th day after IAV infection, significant difference (p<0.05) was found between experimental group and control (n=5/ each group).

ET-1 expression and BBB permeability

To clarify the possible mechanism for ETs on injury, the effects on BBB disruption and edema infiltration were examined. The brain EB level was markedly increased on day 3 and further increased on day 5 after IAV Infection (fig. 2A), indicated that elevating the ET-1 level in damaged and brain edema, mortality, and albumin extravasation reduced by IAV infection (fig. 2B).

INOS expression and edema

Reactive oxygen species (ROS) and reactive nitrogen species (RNS) as mediators of IAV-induces tissue damage have been confirmed in which exogenous antioxidant treatment decreased tissue damage and mortality in fig. 3A. RNS such as nitric oxide (NO) are generated in lung by activated macrophages, neutrophils, type II pneumocytes, airway epithelial cells and iNOS is expressed by inflammatory cytokines damage (fig. 3B).

TNF-α and mitochondria fatty acid metabolism

The cerebral TNF-α level was analyzed and the effect of infection on the metabolism in the brain to examine the pathogenesis of influenza encephalitis in newborn mice. TNF-α level was elevated on day 3 and continued to increase significantly on day 5, especially after diclofenac treatment (fig. 4A). The levels of total-, free-, short chain acyl- and long chain acyl-carnitine in the brains of newborn mice with or without IAV infection on day 5 are shown in fig. 4B.

DISCUSSIONS

Much attention has been paid to the multiple functions of endothelin (ET) isopeptides, potent vasoconstrictors of

Table 1: List of primers used in the present study

Name	Orientation (5'→3')	Sequence (5'→3')	Product size
IAV 1st	Sense	tgaagtgactaatgctactg	578 bp
	Antisence	tcattgtttggcatagtca	
2nd	Sense	gcaactgttacccttatgat	232 bp
	Antisence	acagacccctttacccagggt	
Q-IAV	Sense	tctgcctctcggccaaga	78 bp
	Antisence	ttggcaccgcatgatgtc	
	Probe	ttccaggaaatgacaacagcacagcaa	208 bp
iNOS	Sense	ctttgtgcgaagtgtcagtgg	
	Antisence	ttcttcctgatagaggtggtcc	
ET-1	Sense	ttcccgtgatcttctctctgct	369 bp
	Antisence	ctgcttggcagaaattcca	
GAPDH	Sense	ggctgccatttgcagtggcaa	104 bp
	Antisence	tgccgtgagtggagtcatactg	

IAV, influenza A virus; 1st, the first-stage PCR; 2nd, the second-stage PCR; Q-IAV, quantitative PCR; iNOS, inducible nitric oxide synthase; ET-1, endothelin-1; GAPDH, glyceraldehyde-3-phosphate dehydrogenase.

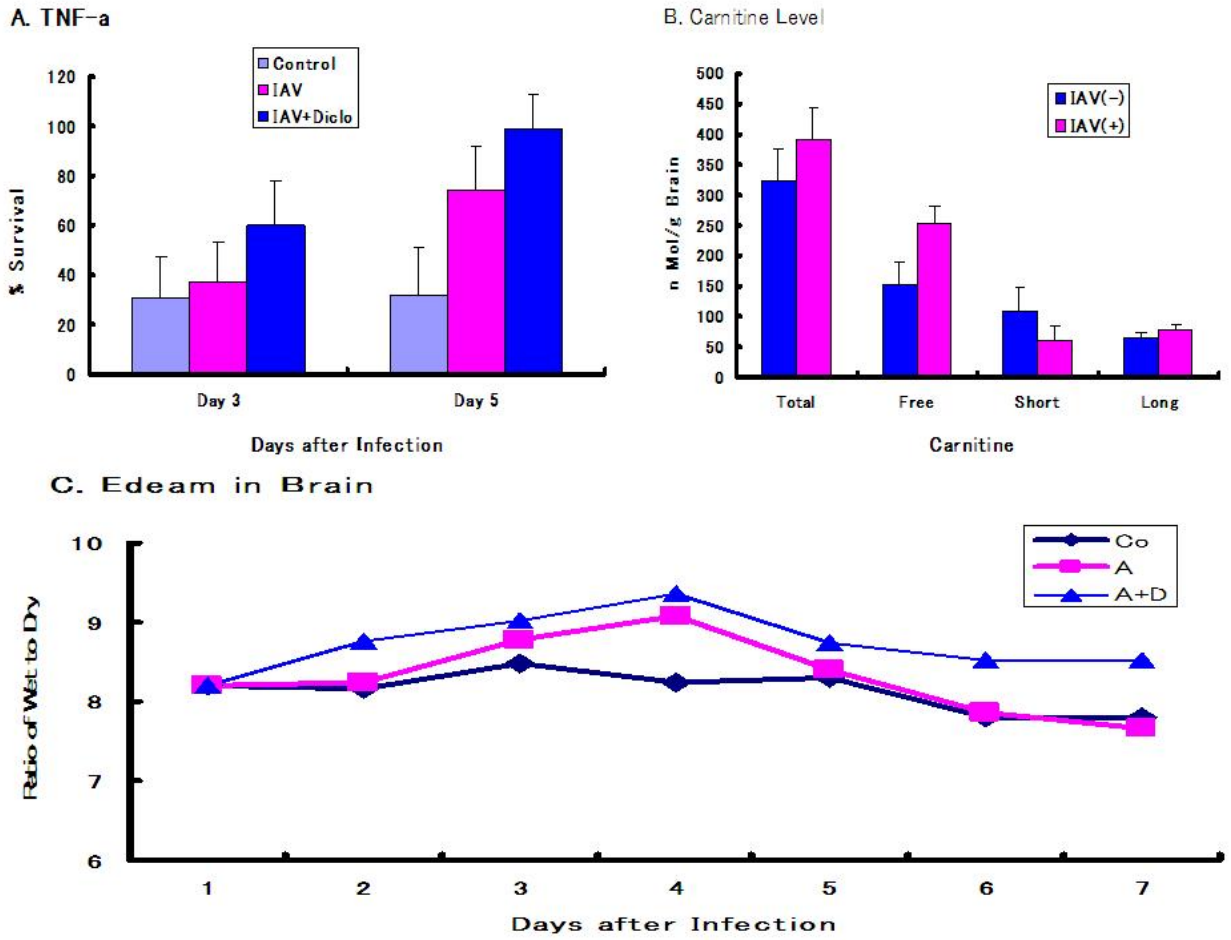

Fig. 4: Expression of TNF-α and change of fatty acid metabolism. A, Level of TNF-α expression in brains of IAV-infected mice was analyzed during experimental period. In brain of IAV-infected mice, slightly increase of TNF-α level was found on day 3 and significant increase on day 5 (p<0.05) in IAV-infected mice only. However, the viral infection mice with diclofenac treatment, the TNF-α level was significantly elevated on day 3 (p<0.05) and 5 (p<0.01). B. Changes of carnitine levels were analyzed on day 5 after IAV infection. After IAV infection, the levels of total carnitine, free carnitine, and long chain acylcarnitine were increased and the short chain acylcarnitine was decreased between experimental group and control. C. Kinetic changes of water content in brain of the viral-infected mice were analyzed at different time. IAV-infected group (■, n=5),IAV-infected with diclofenac treatment group (▲, n=5) and control (◆, n=5). Comparing with the control, the increase of brain water in IAV-infected mice with diclofenac treatment group was found from the 2nd day, highest peak at the 4th day, and then decreasing from the 5th day and persistent higher level until the 7th day. The IAV-infected group only, slight increase of brain water content was found from the 2nd day, highest peak at the 4th day and decreasing to normal level at the 5th day.

vascular smooth muscle, in brain edema formation. In the brain, ETs and their receptors that localize in neurons, glial cells, and smooth muscle cells, and microvessel endothelial cells have been implicated in physiological and pathophysiological roles by modulating neuronal functions and regulation of cerebral blood flow and metabolism (Momtaz S*et al.,* 2010). A marked elevation of brain ET-1 levels has been found and significantly attenuated the brain edema. ET-1 can reduce cerebral blood flow and induce neuronal damage. BBB disruption and edema are induced with the progression of brain injury, suggesting that ETs regulate BBB functions and ET-1 enhances the permeability of BBB as the pathogenesis of brain edema accompanying cerebro-vascular disorders.

Brain water increased slightly but significantly at day 3 and 5, when brain ET-1 level remained unchanged. After 7 days, when a significant increase of ET-1, water began to increase again and continued to rise significantlycontribute to brain edema (Yao *et al*., 2011). It is possible that ET-1 is released from micro-vessels, because the presence of ETs in the endothelial cells. ET localized in neurons and glial cells and glial cells

synthesize ET during active gliosis. A simple explanation would be that it is related to net water uptake because of BBB disruption. Marked elevation in tissue ET-1 levels has been reported in animalcerebral, and there is a tendency of higher ET-1 levels being associated with more severe BBB damage.

It is difficult to determine the individual contributions of the various cytokines produced following IAV infection to pathogenesis, because the cytokines are pleiotropic and redundant in their functions and exert synergistic or antagonistic effects on each other. However, in general, it is believed that among the cytokines produced after IAV, some cytokines like IFN-α/β, IFN-γ, and IL-2 have protective roles against IAV, while some cytokines like IL-1, TNF-α, and IL-6 seem to be involved in the IAV inflammatory phase and abnormal fat metabolism (Yao *et al*., 2008 and Tang *et al.,* 2014).

ACKNOWLEDGMENTS

This work was supported by part grants-in-Aid from the National Natural Science Foundation (81200634, 81370982), the Nantong Undertaking and Technological Innovation (BK2013048, HS2013007, HS2013009), and the Priority Academic Program Development (PADA)of Higher Education Institution of Jiangsu Province, China.

REFERENCES

Cederblad G and Lindstedt S (1972). A method for the determination of carnitine in picomole range. *Clin. Chim. Acta.*, **37**(2): 235-243.

McAuley JL, Tate MD, MacKenzie-Kludas CJ, Pinar A, Zeng W, Stutz A, Latz E, Brown LE and Mansell A (2013). Activation of the NLRP3 inflammasome by IAV virulence protein PB1-F2 contributes to severe pathophysiology and disease. *PLoS. Pathog.*, **9**(5):e1003392.

Momtaz S and Abdollahi M (2010). An update on pharmacology of Satureja species: From antioxidant, antimicrobial, antidiabetes and anti-hyperlipidemic to reproductive stimulation. *Int. J. Pharmacol.,* **6**(4): 454-461.

Sawadogo WR, Boly R, Lompo M, Some N, Lamien CE, Guissou IPand Nacoulma OG (2006). Anti-inflammatory, analgesic and antipyretic activities of *Dicliptera verticillata. Int. J. Pharmacol.*,**2**(4): 435-438.

Tang CC, Lin WL, Lee YJ, Tang YC and Wang CJ (2014). Polyphenol-rich extract of *Nelumbo nucifera* leaves inhibits alcohol-induced steatohepatitis via reducing hepatic lipid accumulation and anti-inflammation in C57BL/6J mice. *Food. Funct.*,**5**(4): 678-687.

Vogel AJ, Harris S, Marsteller N, Condon SA and Brown DM (2014). Early cytokine dysregulation and viral replication are associated with mortality during lethal influenza infection. *Viral. Immunol.*,**27**(5): 214-224.

Yao D, Yao M, Yamaguchi M, Chida J and Kido H (2011).Characterization of compound missense mutation and deletion of carnitine palmitoyltransferase II in a patient with adenovirus-associated encephalopathy. *J. Med. Invest*, **58**(3-4): 210-218.

Yao D, Mizuguchi H, Yamaguchi M, Yamada H, Chida J, Shikata K and Kido H (2008). Thermal instability of compound variants of carnitine palmitoyltransferase II and impaired mitochondrial fuel utilization in influenza-associated encephalopathy. *Hum. Mutat.*, **29**(5): 718-727.

Yao M, Yao D, Yamaguchi M, Chida J, Yao D and Kido H (2011). Bezafibrate up regulates carnitine palmitoyl transferase II expression and promotes mitochondrial energy crisis dissipation in fibroblasts of patients with influenza-associated encephalopathy. *Mol. Genet. Metab.*, **104**(11): 265-272.